Chem Rev Lett 8 (2025) 1146-1154

Research Article

Chemical Review and Letters
journal homepage: www.chemrevlett.com
ISSN (online): 2645-4947 (print) 2676-7279

Electric field-dependent ion selectivity in armchair silicon carbide nanotubes: A molecular dynamics study

Jafar Azamat[1, *]

[1]*Department of Chemistry Education, Farhangian University, P.O. Box 14665-889, Tehran, Iran.*

ARTICLE INFO

Article history:
Received 07 June 2025
Received in revised form 03 August 2025
Accepted 09 August 2025

Keywords:
Molecular dynamics simulations
Silicon carbide nanotube
External electric field
Selectivity
Ion channels

ABSTRACT

Utilizing molecular dynamics simulations, this study investigates the mechanisms underlying the transport of magnesium (Mg^{2+}) and chloride (Cl^{-}) ions through armchair silicon carbide nanotubes (SiCNTs). The simulation framework consisted of a silicon carbide nanotube embedded within a silicon nitride membrane, submerged in an aqueous ionic solution under the influence of an external electric field. Key dynamical and structural properties were analyzed, including ionic current profiles, the potential of mean force, ion retention times within the nanotube, radial distribution functions, and the ratio of water molecules transported relative to ions. The findings reveal a strong correlation between nanotube diameter and ion permeation efficiency, with narrower nanotubes exhibiting distinct selectivity and transport kinetics. This diameter-dependent behavior highlights the potential for tailoring SiCNT dimensions to regulate ion flux. Consequently, the study proposes these nanotube-membrane systems as promising prototypes for the design of biomimetic ion channels or nanofluidic filtration devices. The results underscore the role of nanoscale confinement and electrostatic interactions in modulating ion transport, offering insights for applications in molecular separation technologies and synthetic biological systems.

1. Introduction

Ion movement across cell membranes is regulated by the opening and closing of gated pores, which otherwise act as impermeable barriers to ions [1-3]. Ion channel proteins serve as selective pathways, enabling charged ions to traverse the hydrophobic cell membrane. These channels are dynamic structures that facilitate the generation and regulation of voltage gradients by allowing ions to flow along their electrochemical gradients. In addition to maintaining the cell's electrochemical balance, ion channels play critical roles in rapid physiological processes, including cardiac and skeletal muscle contraction, smooth muscle activity, and the epithelial transport of ions and nutrients.

Notably, silicon carbide nanotubes (SiCNTs) exhibit structural and dimensional similarities to biological ion channels, making them promising candidates for biomimetic applications in nanotechnology [4-8]. Their controllable pore size and ion-selective properties suggest potential uses in synthetic ion channel systems, nanofluidic devices, or next-generation biosensors. SiCNTs represent a relatively recent addition to this family, first synthesized in 2001 [9]. A significant number of theoretical studies have explored their structural characteristics and electronic properties due to their promising behavior and potential applications [10-14]. These nanotubes exhibit versatility in functional use, including roles in catalysis, gas sensing, and ion-selective membrane technologies [15-19].

For instance, Zhao et al. investigated the use of a (8,0) SiC nanotube as a sensor for carbon dioxide, analyzing its response to varying concentrations of CO_2 molecules [15]. In another study, Wang et al. demonstrated the potential of SiC nanotubes as formaldehyde detectors, showing that a notable charge transfer occurs between the nanotube and formaldehyde molecules, enhancing detection sensitivity [20]. Additionally, Zhao et al. proposed that SiC nanotubes could function as efficient catalysts for breaking nitrogen-hydrogen and oxygen-hydrogen bonds without the need for metallic components, opening new avenues in chemical reaction engineering [15]. While carbon nanotubes (CNTs) have been the focus of extensive research, various other

* Corresponding author E-mail: j.azamat@cfu.ac.ir
https://doi.org/10.22034/crl.2025.528864.1625

nanomaterials are also capable of forming tubular nanostructures. These nanostructures, along with boron nitride nanotubes (BNNTs) [21], have garnered substantial interest due to their transformative potential in advancing nanotechnology and mesoscopic science [22, 23]. While CNTs are celebrated for their exceptional electrical conductivity and mechanical resilience, BNNTs represent a distinct class of tubular nanostructures with unique properties. A critical distinction between these nanomaterials lies in their atomic polarization. SiCNTs feature polarized bonds, imparting hydrophilic characteristics, whereas CNTs possess non-polarized bonds and hydrophobic surfaces. This divergence significantly influences their interactions with ions.

In recent years, the study of ion transport mechanisms regulated by ion channels has gained significant momentum, particularly in uncovering the molecular-level interactions that govern selective ion passage [24-26]. Research in this area [27] highlights the crucial role these channels play in various physiological processes. Alongside biological systems, synthetic structures such as nanotubes and artificial nanochannels have emerged as promising candidates for mimicking the functionality of natural ion channels, especially their ability to selectively filter specific ions [28].

Among these synthetic materials, SiC nanotubes have attracted particular interest due to their unique structural and electrochemical properties. Investigations into SiCNT-based ion channels suggest that ion selectivity is strongly influenced by the behavior of water molecules within the confined space of the channel, as well as the surface charge distribution along the channel walls. These findings open new avenues for designing advanced filtration and sensing technologies at the molecular scale.

A variety of computational simulation techniques are available for studying systems across different length scales, ranging from macroscopic [29] to nanoscopic levels [30]. Among these, molecular dynamics (MD) simulations offer a powerful framework for modeling complex phenomena at the molecular scale [31]. One of the key advantages of MD over other computational approaches is its ability to capture dynamic properties of a system, such as time-dependent fluctuations and transport coefficients, which can be derived from time-averaged data [32].

Selective ion transport through nanostructured materials represents a compelling area of research in both chemistry and physics, with implications for applications such as desalination, energy storage, and nanofluidics [33]. In light of this, the present study employs MD simulations to investigate the selective permeation of Mg^{2+} and Cl^{-} ions through armchair SiCNTs under the influence of an external electric field.

To examine the selective transport of magnesium and chloride ions, we utilized SiC nanotubes with (7,7) and (8,8) chiralities, integrated into a silicon nitride membrane [34]. The setup was immersed in a 0.5 M aqueous $MgCl_2$ solution, as illustrated in Figure 1. Each nanotube had a length of approximately 15 Å and their diameter were about 12.26 Å and 13.89 Å, for (7,7) SiCNT and (8,8) SiCNT respectively.

The interaction between the nanotubes and the surrounding membrane environment was modeled by considering both van der Waals and electrostatic forces. Of these, the electrostatic contribution, originating from partial atomic charges present on the surfaces of the SiC nanotubes and the silicon nitride matrix, was found to be particularly significant. These charge-driven interactions are believed to be the primary factor underlying the ion selectivity observed during transport through the nanoscale channels.

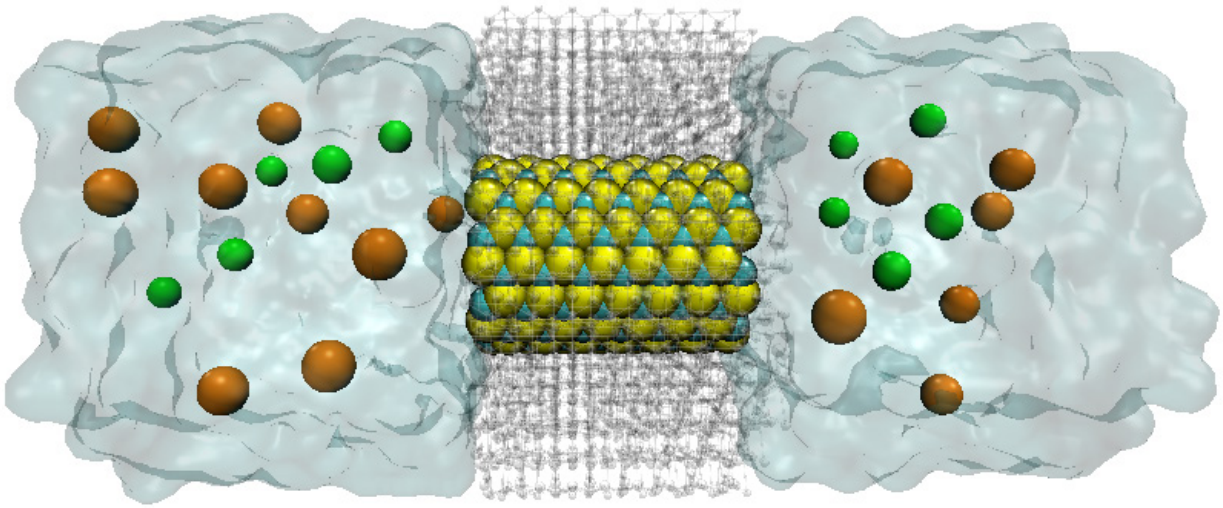

Fig. 1. The (8,8) SiCNT inside a silicon nitride membrane in aqueous solution of $MgCl_2$ (gray: silicon nitride membrane; yellow: silicon; cyan: carbon; green: Mg^{2+}; orange: Cl^{-}).

2. Computational methods

For this study, SiCNTs with (7,7) and (8,8) chiral structures were selected as model systems. The structural optimization of these nanotubes was carried out using the B3LYP functional within the framework of density functional theory (DFT), employing the 6-31G** basis set as implemented in the GAMESS-US software package [35]. This computational approach allows for accurate geometry relaxation by minimizing the total energy of the system. To validate the reliability of the optimized structures, bond lengths were calculated and compared with experimentally reported values for similar SiC-based materials. The resulting Si–C bond length after optimization was found to be approximately 1.8 Å, which is consistent with previously published data.

The non-bonded interactions were modeled using the 12-6 Lennard-Jones potential to account for long-range van der Waals forces [36]. Lennard-Jones parameters for the SiC nanotube were obtained from [25]. Interactions between different atom types, such as those between the nanotube, water molecules, and ions, were determined using the Lorentz-Berthelot mixing rules, ensuring a consistent and transferable force field description across the simulation system.

MD simulations were carried out using the NAMD software package [37], employing a time step of 1 femtosecond. Non-bonded interactions, specifically van der Waals forces, were calculated with a cutoff distance of 12 Å. Electrostatic interactions were treated using the Particle Mesh Ewald (PME) method to ensure accuracy in long-range interactions. The simulation systems were visualized and analyzed using VMD [38].

Each simulation setup included either a SiCNT embedded in a silicon nitride membrane, surrounded by water molecules and ions-specifically magnesium or chloride ions. To incorporate SiCNTs into the SiN membrane, a hole of appropriate size was created at the center of the membrane. This allowed the nitrogen and silicon atoms of the SiN membrane to interact with the (7,7) and (8,8) SiCNTs.

However, not all configurations exhibited ion selectivity. In the optimized system, the diameter of the hole was matched to that of the nanotubes. As a result, nitrogen atoms from the membrane preferentially surrounded the (7,7) SiCNT, while silicon atoms aligned around the (8,8) SiCNT. This specific atomic arrangement facilitated selective ion transport, enabling the system to effectively separate ions from water.

The entire system was solvated within a rectangular simulation box measuring approximately 36×42×51 Å^3 and was periodically replicated in all three spatial dimensions to mimic bulk behavior. A uniform electric field was applied throughout the simulation domain for all studied systems to induce ion transport and examine electrophoretic behavior over time. For the simulations, the CHARMM27 force field [39] was used to model the interactions of all organic and inorganic components. The TIP3P model [40] was selected to describe the water molecules due to its compatibility with the CHARMM parameter set. Although newer models like TIP4P offer improved diffusion properties, they are more computationally intensive and not always necessary depending on the focus of the study. The TIP3P model has been widely validated and demonstrates good agreement with experimental data in terms of structural and thermodynamic characteristics. Compared to SPC-type water models, which are primarily optimized for use with the GROMOS force fields, TIP3P provides a more accurate representation of water's physical properties when used in conjunction with CHARMM-based simulations.

Initially, energy minimization was performed over 100,000 time steps at 0 Kelvin to eliminate unfavorable conformations. Subsequently, a gradual temperature ramping was applied, increasing the system temperature to 310 K over 50,000 time steps. Finally, a range of electrical fields, from 0.5 (kcal/mol·Å·e) to 5 (kcal/mol·Å·e), was applied along the z-direction to drive ions transport through the nanotubes during 5 ns MD simulations.

Temperature control was achieved using a Langevin thermostat, while pressure regulation was maintained via a hybrid Nosé-Hoover Langevin piston method. During both equilibration and production phases, the silicon nitride membrane and the SiC nanotubes were kept structurally stable through the application of harmonic restraints. In contrast, water molecules and ions were allowed to move freely to ensure realistic dynamic behavior. These positional constraints were introduced specifically to preserve the structural integrity of the membrane and to align its dielectric properties with experimentally reported values. Without such restraints, the membrane tends to collapse or deform significantly during the simulation, which would render the system physically unrealistic.

To investigate ion transport behavior, current–electric field relationships were computed for all systems at an ionic concentration of 0.5 M, based on simulation outcomes. The electric current was calculated using the following expression, $I = q.n/\Delta t$, where n represents the average number of ions translocating through the nanotube per simulation run, q is the charge of a single ion, and Δt denotes the total simulation time.

The observed differences in ion selectivity among the SiCNTs were further analyzed by computing the potential of mean force (PMF) along the transport pathway. This was accomplished using umbrella sampling simulations, followed by data processing with the weighted histogram analysis method. In these calculations, individual ions were pulled along the axial direction (z-axis) of the nanotube from 0 to 15 Å in increments of 0.5 Å. A harmonic biasing potential with a force constant of 12.5

kcal/mol·Å^{-2} was applied along the z-direction to maintain sampling windows, while allowing full radial mobility. The chosen restraint strength ensured sufficient overlap between adjacent sampling windows, thereby enabling accurate reconstruction of the free energy profile across the entire reaction coordinate.

3. Results and Discussion

To investigate various transport and structural properties, such as ionic current, hydrogen bonding patterns, normalized water transport rate relative to ion flux, ion residence time, and ion-water radial distribution functions, MD simulations were conducted. These simulations enabled the examination of both dynamic and energetic behaviors of the system, allowing for a comprehensive understanding of ion and water transport mechanisms through the nanotubes.

The system was simulated for a sufficient time to reach a steady state, ensuring that all structural, geometric, and energetic characteristics stabilized. This allowed for accurate measurement of key parameters under equilibrium conditions. Monitoring the total energy of the system, along with hydrogen bond formation and other structural indicators, confirmed that the simulations had indeed reached a stable state.

Figure 2 presents the radial distribution functions (RDFs) between water molecules and the nanotube surface. The RDF plots provide insight into the density profile of water near the nanotube walls. Water molecules adopt a highly ordered, cylindrical configuration within the confined space of the nanotubes, which is consistent with the RDF data indicating strong interactions between the water and the inner surface of the nanotubes.

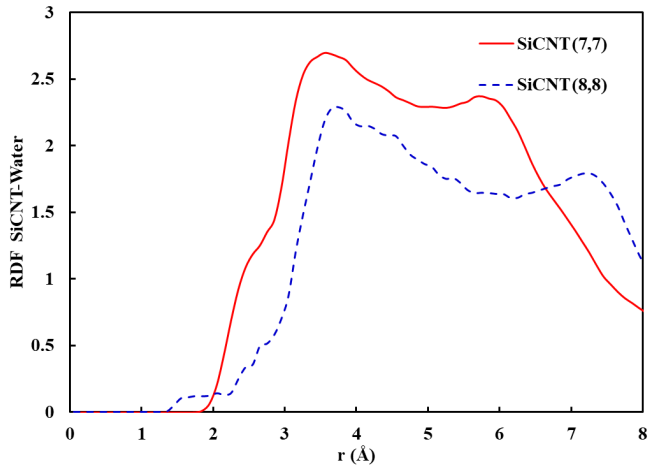

FiG. 2. The position of water molecules inside (7,7) and (8,8) SiCNTs.

In particular, the RDF analysis for the (7,7) nanotube reveals a distinct shift of the first peak toward smaller distances compared to the (8,8) nanotube. This suggests a closer proximity of water molecules to the nanotube wall in the narrower tube. Additionally, the increased intensity of this peak implies stronger localization and enhanced interaction between the water molecules and the nanotube surface in this configuration. These observations highlight how nanotube geometry influences the structure and behavior of confined water, which in turn affects ion transport and selectivity.

Despite the nanotubes having a sufficiently large radius to accommodate both magnesium and chloride ions, MD simulations reveal that Mg^{2+} ions selectively pass through (7,7) nanotubes, whereas Cl^- ions preferentially permeate through (8,8) nanotubes. This distinct ion selectivity arises due to differences in the alignment of water molecule dipole moments within the nanotubes, which in turn influence the internal electric field distribution. To better understand this phenomenon, we conducted MD simulations to investigate the orientation of water dipoles confined inside these nanotubes over the course of the simulation. The dipole orientation is characterized by the angle formed between the dipole vector of each water molecule and the central axis of the nanotube.

The results indicate that water molecules inside (7,7) nanotubes exhibit dipole moments predominantly aligned toward the tube's axis, while those within (8,8) nanotubes show an upward orientation relative to the axis. These contrasting dipole alignments are attributed to the nature of the atoms lining the membrane around each nanotube type. Specifically, nitrogen atoms of the membrane, carrying a partial negative charge of –0.593e surround the (7,7) nanotubes, whereas silicon atoms of the membrane, with a partial positive charge of +0.771e encircle the (8,8) nanotubes. This variation in atomic composition leads to distinct electrostatic environments, thereby influencing the behavior of confined water and ion transport properties.

To understand the thermodynamic underpinnings of ion selectivity in silicon carbide nanotubes (SiCNTs), we calculated the potentials of mean force (PMF), which quantify the free energy landscape an ion experiences as it traverses the axial (z) direction of the nanotube pore. PMFs provide critical insights into the energetic favorability or resistance an ion encounters at each point along its path, encompassing both enthalpic and entropic contributions arising from ion–pore and ion–solvent interactions.

These PMF profiles are presented in Figure 3 for the systems under investigation. As shown in this figure, the (7,7) nanotube imposes a significant energy barrier against the transport of chloride (Cl^-) ions. This barrier likely arises from electrostatic repulsion between the negatively charged ion and the partial charges or polar environment at the nanotube wall, compounded by the disruption of the Cl^- hydration shell in the confined geometry. The energetic penalty for dehydrating or distorting the hydration structure as the ion enters the narrow pore region contributes to this unfavorable free

energy. Conversely, in the (8,8) nanotube, a similar energy barrier is observed, but it primarily impedes the transport of divalent magnesium (Mg^{2+}) ions. Mg^{2+}, due to its smaller ionic radius and higher charge density, forms a more tightly bound and structured hydration shell compared to Cl^{-}. The desolvation of Mg^{2+} as it moves through the pore is energetically more costly, especially when the pore diameter approaches the size of the hydrated ion complex.

Interestingly, in both nanotube types, the PMF curves exhibit a pronounced energy minimum near the center of the pore. This minimum indicates a metastable binding site where ions can become temporarily trapped. The stabilization at this position is likely due to favorable electrostatic interactions and the formation of a structured hydrogen-bond network involving confined water molecules. These interactions reduce the local free energy, effectively creating a potential well that promotes transient ion localization, which may influence both ion permeation rates and selectivity.

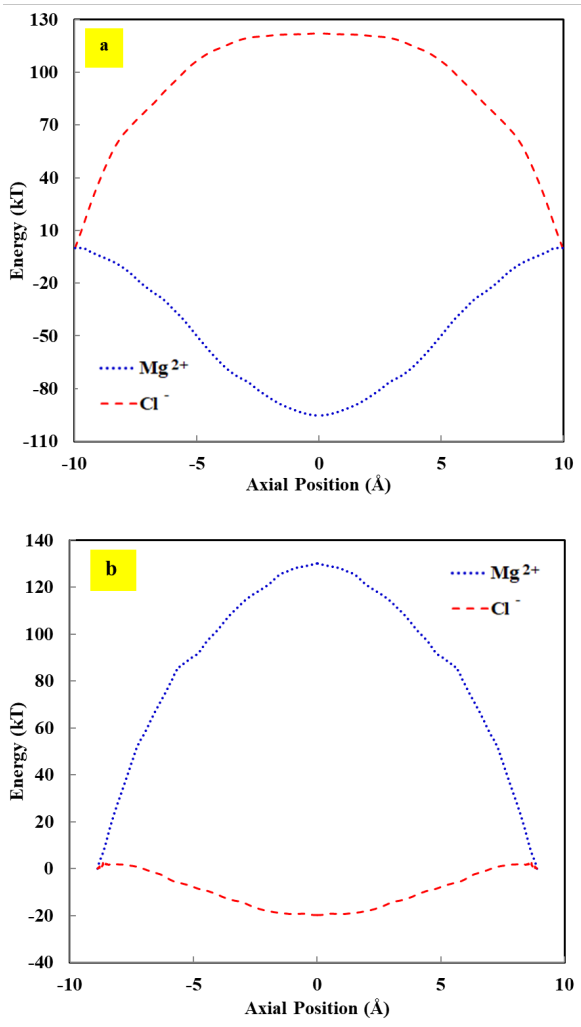

Fig. 3. PMF for Mg^{2+} and Cl^{-} ions in (a): SiCNT (7, 7) and (b): SiCNT (8, 8).

The PMF calculations were carried out in the absence of an external electric field. Under these conditions, ions tend to enter the nanotube and accumulate around the central region. However, when an electric field is applied, the ions gain sufficient energy to overcome the potential barrier, allowing them to traverse the pore and exit the nanotube.

The PMF reflects how the free energy changes as a function of selected degrees of freedom; in this case, the position of an ion relative to the center of the nanotube along its axial direction. When the PMF increases with displacement, it indicates that movement in that direction is energetically unfavorable, meaning transport will not occur spontaneously. In our simulations, the PMF rises near the pore entrances and reaches its peak at the center of the nanotube, as illustrated in Figure 3. This trend can be attributed to the system's high symmetry and the complex interplay between ions, the nanotube structure, and the surrounding membrane. This behavior aligns well with the simulation results showing that anions are largely excluded from entering the (7,7) nanotube. Furthermore, the increase in PMF primarily stems from the interactions between the ions and the nanotube-membrane environment. In contrast, the influence of water molecules on the free energy profile within the pore appears to be minimal.

The selectivity between cations and anions is strongly influenced by the dipole moment surrounding the nanotube. In the case of a (7,7) nanotube embedded in a silicon nitride membrane, the silicon atoms on the nanotube surface are slightly displaced outward due to interactions with nitrogen atoms from the surrounding matrix, which are located on the exterior side of the pore. Conversely, in (8,8) nanotubes, the situation is reversed: the carbon atoms of the nanotube move outward relative to the boron atoms. This structural shift occurs because the nanotube is encircled by silicon atoms from the membrane, which exert different electrostatic and structural influences compared to the nitrogen-rich environment of the (7,7) configuration.

Figure 4 presents the relationship between the ionic current and the applied electric field. The resulting curve demonstrates a linear dependence, indicating that the flow of ions through the nanotube increases proportionally with the strength of the electric field. This linear behavior suggests a steady and predictable enhancement in transport efficiency as the driving force is increased.

The rate of water transport through the nanotubes is calculated as the average number of water molecules that pass through the pore divided by the total simulation time. This metric has been extracted from the simulations and is illustrated in Figures 5(a) and 5(b), which show both the absolute water transport rate and the normalized water transport rate, defined as the number of water molecules transported per permeating ion. The results indicate that the normalized transport rate remains constant regardless of the strength of the applied electric field. This suggests

that the coupling between ion and water transport is consistent under varying field conditions.

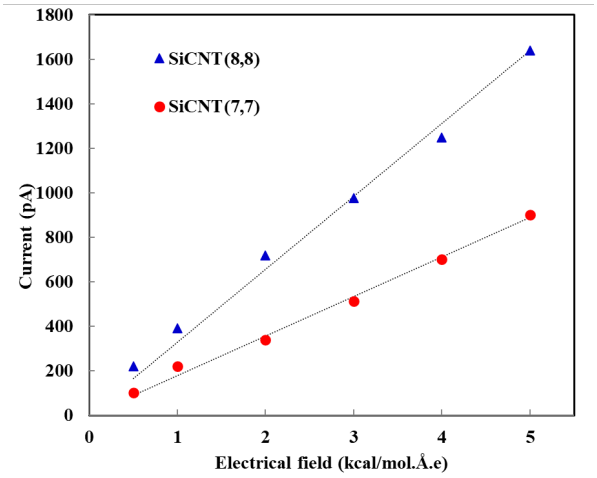

Fig. 4. Current-electrical field curve for Mg^{2+} ion in (7,7) SiCNT and Cl^- ion in SiCNT (8,8); lines have been obtained from a linear regression.

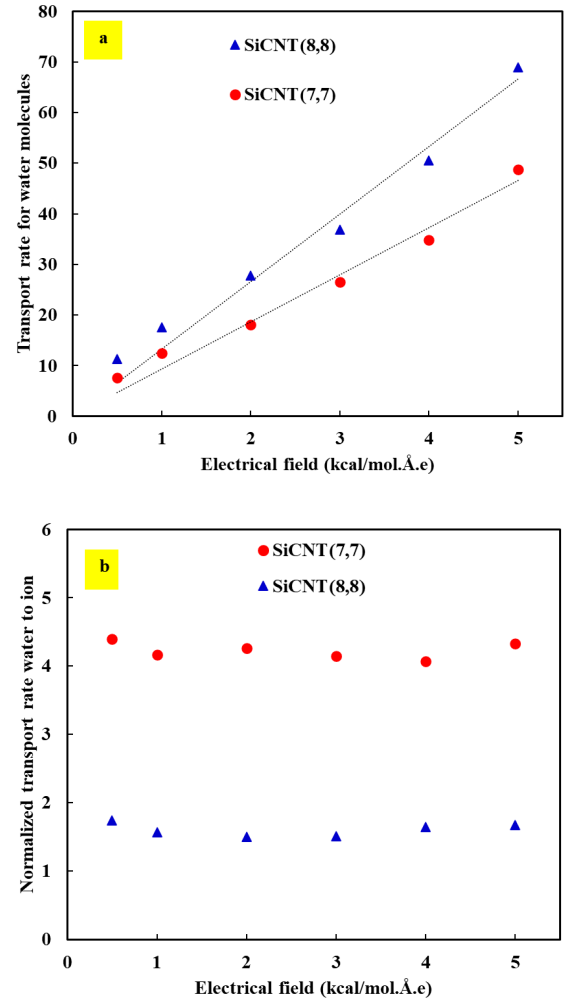

Fig. 5. (a) Transport rate for water molecules; lines have been obtained from a linear regression. (b) Normalized transport rate water to ion.

Table 1 presents the retention time, the duration an ion remains inside a nanotube, as it varies with the applied electric field. As the strength of the electric field increases, the retention time of ions decreases. The data also indicate that boron nitride nanotubes exhibit longer retention times compared to other types, suggesting stronger interactions between the ions and the nanotube surface.

Table 1. Retention time (ns) of ions for each applied electrical field.

Electrical field (*kcal/mol·Å·e*)	Mg^{2+}	Cl^-
	SiCNT (7,7)	SiCNT (8,8)
0.5	0.0986	0.0654
1	0.0788	0.0437
2	0.0511	0.021
3	0.0305	0.0109
4	0.0159	0.0053
5	0.0091	0.0019

MD simulations revealed distinct water organization within the SiCNTs depending on their diameter. Inside the (7,7) SiCNT, water molecules formed a cylindrical arrangement with a single-file structure, whereas in the (8,8) SiCNT, water adopted a more complex configuration consisting of two concentric cylindrical layers. Despite these ordered structures, the movement of water through the nanotubes did not follow a consistent directional pattern. The presence of ions was found to disrupt the structured arrangement of water, primarily through the formation of hydrogen bonds between water molecules and the ions. This interaction led to a fragmentation or "splintering" of the otherwise ordered water structure.

Figure 6 presents the total number of hydrogen bonds formed between water molecules under different electric field strengths for both (7,7) and (8,8) SiC nanotubes. The data indicate that the number of hydrogen bonds increased with the magnitude of the applied electric field. This trend was further validated by analyzing the normalized hydrogen bond count relative to the number of water molecules confined inside the nanotubes, as shown in Figure 7. For instance, in the (8,8) SiC nanotube, the normalized hydrogen bond value rose with increasing electric field intensity but declined as temperature increased, suggesting a thermal disruption of hydrogen bonding. Figure 8 illustrates the radial distribution functions (RDFs) characterizing ion–water interactions within silicon carbide nanotubes (SiCNTs) under varying externally applied electric fields. Specifically, Figure 8(a) presents the Mg^{2+}–water RDF inside a (7,7) SiCNT, while Figure 8(b) shows the Cl^-–water RDF within an (8,8) SiCNT. RDFs describe how particle density varies as a function of distance from a reference particle—in this case, the ion—and are useful in assessing the degree of local structural ordering in molecular systems.

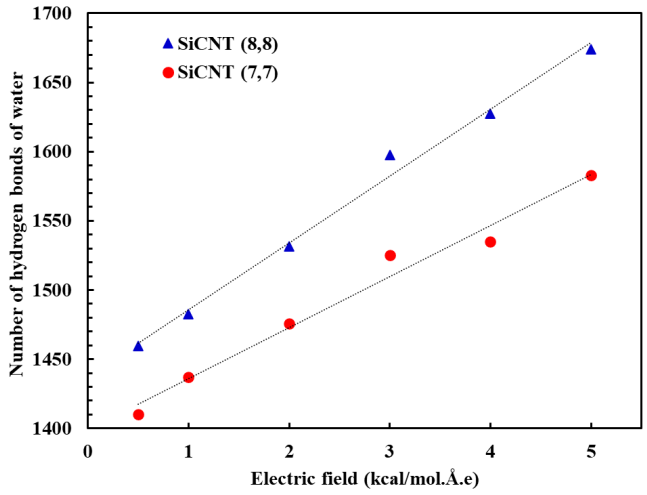

Fig. 6. The number of hydrogen bonds between water molecules of the whole system in the applied electric fields for (7,7) and (8,8) SiCNT. Lines have been obtained from a linear regression.

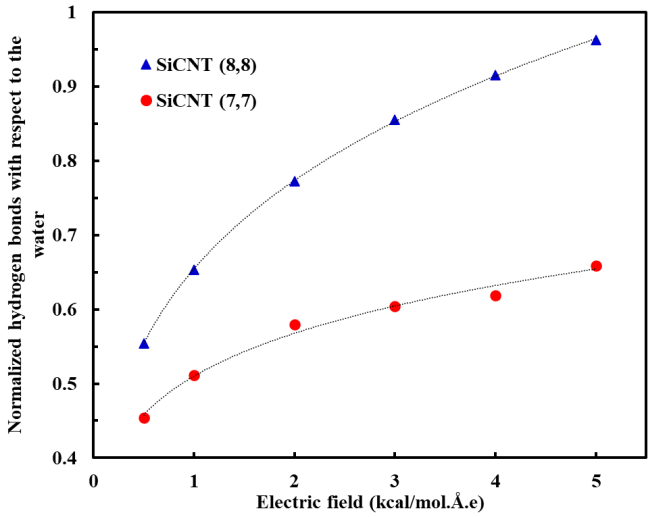

Fig. 7. The normalized hydrogen bonds for the (7,7) and (8,8) SiCNT with respect to the number of inner water molecules.

Distinct changes in the RDF profiles are evident as the strength of the electric field varies. These differences can be attributed to the influence of the electric field on ion dynamics, particularly the retention time—the average duration that ions remain confined within the nanotube environment. At lower electric field strengths, the driving force on the ions is relatively weak, resulting in slower ion mobility. This slower movement allows the surrounding water molecules to reorient and organize more thoroughly around the ion, forming a well-defined hydration shell. As a result, the RDF exhibits sharper and more pronounced peaks, indicating strong local structuring.

In contrast, higher electric field strengths impart greater kinetic energy to the ions, increasing their mobility and decreasing their residence time within the nanotube. This reduced interaction time disrupts the stable arrangement of water molecules around the ion, leading to a less organized hydration structure. Consequently, the RDF becomes broader and less distinct, reflecting diminished spatial correlations between the ion and surrounding water molecules. This behavior illustrates the dynamic coupling between ion transport and hydration structure under confinement and external stimuli.

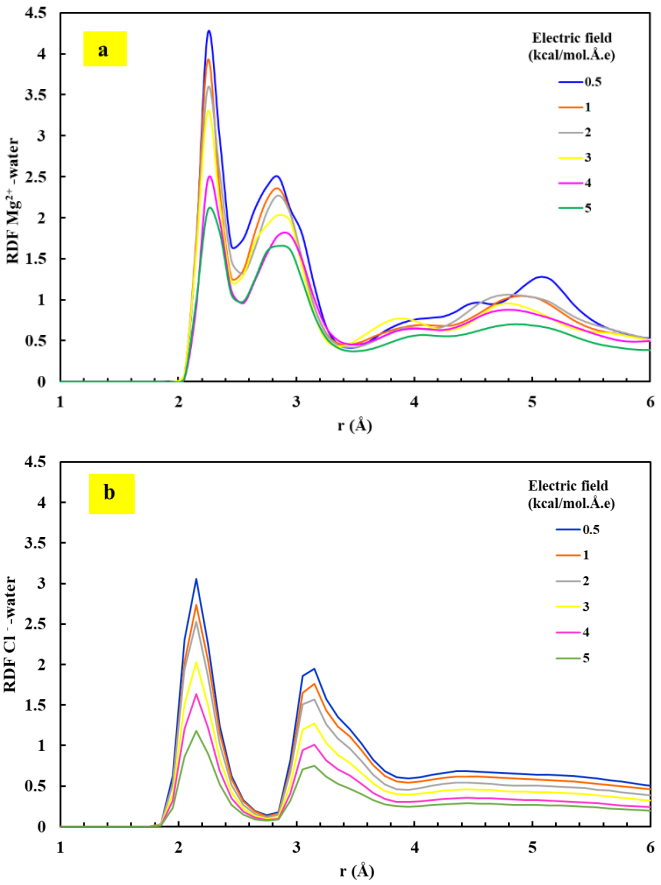

Fig. 8. RDF for ion-water inside the nanotubes at various electrical field: (a) Mg^{2+} in SiCNT (7, 7), (b) Cl^{-} in SiCNT (8, 8).

A detailed comparison between Table 1 and Figure 8 reveals a clear correlation between the height of the RDF peaks and ion retention times. Specifically, nanotubes exhibiting higher RDF peak intensities correspond to conditions of longer retention times, which occur at lower electric fields. This indicates that increased ion confinement enhances the structural organization of the surrounding water molecules, resulting in a more defined hydration shell.

At lower electric field strengths, the retention times of ions exhibit some overlap, suggesting that ion transport is not entirely independent. This implies that under weak fields, an ion may enter the nanotube and remain inside until another ion enters, potentially facilitating its exit. However, at higher electric fields, this overlap disappears, indicating that ions traverse the nanotube individually, without relying on interactions with other ions. This difference in behavior can be attributed to the

presence of a stable binding region at the center of the nanotube under low-field conditions. In such cases, ions tend to dwell in this region, resulting in extended retention times. Conversely, when the electric field is strong, this binding effect is suppressed, and ions pass through the nanotube without significant stay or interaction.

Figure 9 illustrates the *z*-positions of chloride ions (Cl^-) during simulations conducted under two distinct electric field strengths (2 and 5 kcal/mol·Å·e) for the (8,8) SiCNT system. Under both low and high electric fields, a Cl^- ion was able to enter the nanotube. However, in the case of the lower electric field, the ion remained trapped inside unless a second ion entered, providing the necessary electrostatic push for the first ion to exit. In contrast, under the higher electric field, ions were able to pass through the nanotube independently and without such assistance. Furthermore, while the *z*-positions of Cl^- ions showed overlapping trajectories under the low electric field, indicating hindered movement, no such overlap was observed under the high electric field, suggesting more directed and efficient ion transport.

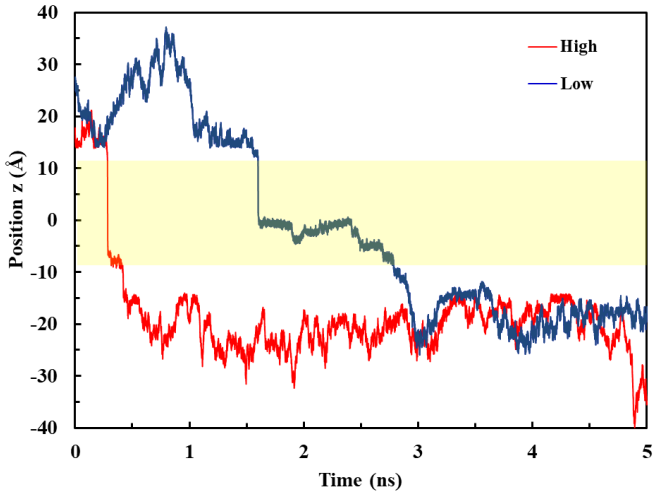

Fig. 9. The z-position of Cl^- in the (8,8) SiCNT during the simulation time in the low electric field (2 kcal/mol·Å·e) and high electric field (5 kcal/mol·Å·e). The highlighted section shows the membrane.

4. Conclusion

This study investigated the selective transport of Mg^{2+} and Cl^- ions through armchair SiCNTs with (7,7) and (8,8) chiralities under various external electric fields using MD simulations. The SiCNTs were embedded in a silicon nitride membrane and exposed to an aqueous $MgCl_2$ solution under applied electric fields. Key properties such as ionic current, ion retention time, water transport rate, PMF, and ion–water radial distribution functions were analyzed to understand the underlying mechanisms of ion permeation and selectivity.

The results demonstrated that ion selectivity is strongly influenced by the diameter and surface charge distribution of the nanotubes. Specifically, Mg^{2+} ions preferentially permeated through the narrower (7,7) nanotube, while Cl^- ions showed higher permeability through the wider (8,8) nanotube. This behavior was attributed to differences in the orientation of water dipoles inside the nanotubes, which are influenced by the local electrostatic environment created by the surrounding membrane atoms.

Moreover, the presence of distinct energy barriers and binding sites within the nanotubes, as revealed through PMF calculations, further supported the observed selectivity. At lower electric fields, ions exhibited longer retention times and formed more structured hydration shells, as evidenced by sharper RDF peaks and reduced hydrogen bond disruption. In contrast, higher electric fields reduced ion dwell time and weakened hydration structures, allowing for faster but less selective ion transport. These findings highlight the potential of silicon carbide nanotubes as biomimetic ion channels or components of nanofluidic devices. Their ability to selectively regulate ion flow based on size, charge, and electric field conditions offers valuable insights for applications in molecular separation, synthetic biology, and advanced filtration technologies.

Acknowledgements

This work received financial support from the Farhangian University (Contract No. 50000/15186/120).

References

[1] J. Kulbacka, A. Choromańska, J. Rossowska, J. Wężgowiec, J. Saczko, M.-P. Rols, Cell Membrane Transport Mechanisms: Ion Channels and Electrical Properties of Cell Membranes. In: *Transport Across Natural and Modified Biological Membranes and its Implications in Physiology and Therapy*, J. Kulbacka, S. Satkauskas (Eds.), Springer International Publishing, Cham (2017) pp. 39-58.

[2] D. Zabelskii, S. Bukhdruker, S. Bukhalovich, F. Tsybrov, G. H. U. Lamm, R. Astashkin, et al., Ion-conducting and gating molecular mechanisms of channelrhodopsin revealed by true-atomic-resolution structures of open and closed states. *Nat. Struct. Mol. Biol.*, 32 (2025) 141-150.

[3] L. Catacuzzeno, A. Michelucci, F. Franciolini, The crucial decade that ion channels were proven to exist. *Pflüg. Arch. Eur. J. Physiol.*, 477 (2025) 903-917.

[4] P. Li, P. Galek, J. Grothe, S. Kaskel, Carbon-based iontronics – current state and future perspectives. *Chem. Sci.*, 16 (2025) 7130-7154.

[5] T. Zhang, L. Li, X. Sun, Y. Shi, W. Cheng, L. Pan, Recent advances in nanomaterials for wearable devices: classification, synthesis, and applications. *Nanotechnology*, 36 (2025) 232003.

[6] J. Azamat, A. Khataee, Separation of CH_4/C_2H_6 mixture using functionalized nanoporous silicon carbide nanosheet. *Energy Fuels*, 32 (2018) 7508-7518.

[7] A. Khataee, G. Bayat, J. Azamat, Molecular dynamics simulation of salt rejection through silicon carbide

nanotubes as a nanostructure membrane. *J. Mol. Graph. Model.*, 71 (2017) 176-183.
[8] A. Khataee, J. Azamat, G. Bayat, Separation of nitrate ion from water using silicon carbide nanotubes as a membrane: Insights from molecular dynamics simulation. *Comput. Mater. Sci.*, 119 (2016) 74-81.
[9] C. Pham-Huu, N. Keller, G. Ehret, M. J. Ledoux, The first preparation of silicon carbide nanotubes by shape memory synthesis and their catalytic potential. *J. Catal.*, 200 (2001) 400-410.
[10] M. Menon, E. Richter, A. Mavrandonakis, G. Froudakis, A. N. Andriotis, Structure and stability of SiC nanotubes. *Phys. Rev. B*, 69 (2004) 115322.
[11] Y. Zhang, H. Huang, Stability of single-wall silicon carbide nanotubes–molecular dynamics simulations. *Comput. Mater. Sci.*, 43 (2008) 664-669.
[12] A. Mavrandonakis, G. E. Froudakis, M. Schnell, M. Mühlhäuser, From pure carbon to silicon-carbon nanotubes: An ab-initio study. *Nano Lett.*, 3 (2003) 1481-1484.
[13] T. Taguchi, N. Igawa, H. Yamamoto, S. Jitsukawa, Synthesis of silicon carbide nanotubes. *J. Am. Ceram. Soc.*, 88 (2005) 459-461.
[14] D. Bai, Size, morphology and temperature dependence of the thermal conductivity of single-walled silicon carbide nanotubes. *Fuller. Nanotub. Carbon Nanostruct.*, 19 (2011) 271-288.
[15] J.-x. Zhao, Y.-h. Ding, Can silicon carbide nanotubes sense carbon dioxide? *J. Chem. Theory Comput.*, 5 (2009) 1099-1105.
[16] J. Azamat, M. R. Khodadust, A. Bahrami Maddah, The role of technical English proficiency in chemistry education. *Chem. Rev. Lett.*, 7 (2024) 731-741.
[17] Y. Jia, G. Zhuang, J. Wang, Electric field induced silicon carbide nanotubes: a promising gas sensor for detecting SO_2. *J. Phys. D: Appl. Phys.*, 45 (2012) 065305.
[18] J. Azamat, The role and importance of observing safety principles in laboratory work. *Res. Chem. Educ.*, 5 (2024) 30-42.
[19] A. Khataee, G. Bayat, J. Azamat, Separation of cyanide from an aqueous solution using armchair silicon carbide nanotubes: insights from molecular dynamics simulations. *RSC Adv.*, 7 (2017) 7502-7508.
[20] X. Wang, K. M. Liew, Silicon carbide nanotubes serving as a highly sensitive gas chemical sensor for formaldehyde. *J. Phys. Chem. C*, 115 (2011) 10388-10393.
[21] A. Rubio, J. L. Corkill, M. L. Cohen, Theory of graphitic boron nitride nanotubes. *Phys. Rev. B*, 49 (1994) 5081-5084.
[22] J. Azamat, A. Khataee, S. W. Joo, Separation of a heavy metal from water through a membrane containing boron nitride nanotubes: molecular dynamics simulations. *J. Mol. Model.*, 20 (2014) 2468.
[23] J. Azamat, A. Khataee, S. W. Joo, Removal of heavy metals from water through armchair carbon and boron nitride nanotubes: a computer simulation study. *RSC Adv.*, 5 (2015) 25097-25104.
[24] K. Malek, M. Sahimi, Molecular dynamics simulations of adsorption and diffusion of gases in silicon-carbide nanotubes. *J. Chem. Phys.*, 132 (2010) 014701.
[25] F. Taghavi, S. Javadian, S. M. Hashemianzadeh, Molecular dynamics simulation of single-walled silicon carbide nanotubes immersed in water. *J. Mol. Graph. Model.*, 44 (2013) 33-43.
[26] D. Jahanshahi, O. Mehdi, V. Esmail, J. Azamat, Performance of silicon carbide nanomaterials in separation process. *Sep. Purif. Rev.*, 52 (2023) 205-220.
[27] T. Lu, A. Y. Ting, J. Mainland, L. Y. Jan, P. G. Schultz, J. Yang, Probing ion permeation and gating in a K+ channel with backbone mutations in the selectivity filter. *Nat. Neurosci.*, 4 (2001) 239-246.
[28] D. Stein, M. Kruithof, C. Dekker, Surface-charge-governed ion transport in nanofluidic channels. *Phys. Rev. Lett.*, 93 (2004) 035901.
[29] R. Saghatchi, J. Ghazanfarian, M. Gorji-Bandpy, Numerical simulation of water-entry and sedimentation of an elliptic cylinder using smoothed-particle hydrodynamics method. *J. Offshore Mech. Arct. Eng.*, 136 (2014) 031801.
[30] A. Zen, Y. Luo, G. Mazzola, L. Guidoni, S. Sorella, Ab initio molecular dynamics simulation of liquid water by quantum Monte Carlo. *J. Chem. Phys.*, 142 (2015) 144111.
[31] D. C. Rapaport, *The Art of Molecular Dynamics Simulation*, 2nd ed. Cambridge University Press, Cambridge (2004).
[32] H. C. Andersen, Molecular dynamics simulations at constant pressure and/or temperature. *J. Chem. Phys.*, 72 (1980) 2384-2393.
[33] K. Al-Khaza'leh, J. A. Talla, M. A. Salem, Effect of external electric field on the electronic and magnetic properties of doped silicon carbide nanotubes: DFT. *Appl. Phys. A*, 129 (2023) 251.
[34] J. K. Holt, A. Noy, T. Huser, D. Eaglesham, O. Bakajin, Fabrication of a carbon nanotube-embedded silicon nitride membrane for studies of nanometer-scale mass transport. *Nano Lett.*, 4 (2004) 2245-2250.
[35] M. W. Schmidt, K. K. Baldridge, J. A. Boatz, S. T. Elbert, M. S. Gordon, J. H. Jensen, et al., General atomic and molecular electronic structure system. *J. Comput. Chem.*, 14 (1993) 1347-1363.
[36] C. Y. Won, N. R. Aluru, Water permeation through a subnanometer boron nitride nanotube. *J. Am. Chem. Soc.*, 129 (2007) 2748-2749.
[37] L. Kalé, R. Skeel, M. Bhandarkar, R. Brunner, A. Gursoy, N. Krawetz, et al., NAMD2: Greater scalability for parallel molecular dynamics. *J. Comput. Phys.*, 151 (1999) 283-312.
[38] W. Humphrey, A. Dalke, K. Schulten, VMD: Visual molecular dynamics. *J. Mol. Graphics*, 14 (1996) 33-38.
[39] B. R. Brooks, R. E. Bruccoleri, B. D. Olafson, D. J. States, S. Swaminathan, M. Karplus, CHARMM: A program for macromolecular energy, minimization, and dynamics calculations. *J. Comput. Chem.*, 4 (1983) 187-217.
[40] W. L. Jorgensen, J. Chandrasekhar, J. D. Madura, R. W. Impey, M. L. Klein, Comparison of simple potential functions for simulating liquid water. *J. Chem. Phys.*, 79 (1983) 926-935.